



# POWER INJECTION STRATEGIES FOR THREE-PHASE FOUR-WIRE INVERTERS DURING VOLTAGE SAGS BY USING FUZZY LOGIC CONTROLLER

(K.SreekanthReddy<sup>1</sup> Dr.E.Kiran Kumar<sup>2</sup>)

<sup>1</sup>(M.Tech Student, Dept. of Electrical and Electronics Engineering, Swetha Institute of Technology and Science, India)

Email Id: sreekanthreddykogatam@gmail.com

<sup>2</sup>(Professor, Dept. of Electrical and Electronics Engineering, Swetha Institute of Technology and Science, India)

Email Id: endala.kirankumar@gmail.com

## Abstract –

It is predicted that electric grid codes will alter in Close future to handle an increased number of In the distribution power unit, distributed generation units Device without impairing its quality of power. It is sought after that the generators remain connected during sags of voltage and provide ancillary services, such as reactive and voltage, Power management, ensuring the functional reliability of the System of influence. This paper examines how to characterize the present Active and Reactive Power Injection Affect Strategies the operation of grid-tied inverters as needed in terms of Energy, current flow, and active power reduction During the Voltage Sags, delivery. In addition, this paper contributes to devise 1) constant peak current control, 2) constant active current control and 3) constant average active power control strategies for three-phase four-wire grid-tied inverters considering the natural (*abc*) reference frame. The proposed system is controlled by using Fuzzy Logic Controller as the response of FLC is quick compared to PI Controller. The layout and implementation of the investigated power injection Strategies and their performance and effectiveness are debated, and Functional feasibility is evaluated by dynamic analysis. Computational simulations are carried out under Sags of symmetrical/asymmetrical voltage, and variance of Ratio of short-circuit.

## I. INTRODUCTION

Advances on power gadgets innovation related with value decreases of photovoltaic (PV) boards, and the appropriation of feed-in duty strategies in numerous nations have added to the boundless utilization of

disseminated generators (DGs). In any case, the high infiltration level of DG can introduce negative effects on the force network in the event that it isn't trailed by cutting edge control procedures in consistence with matrix necessities [1]. During typical voltage condition, low-voltage PV based DG frameworks work with solidarity power factor following the most extreme force point [2]. In light of irregular lattice conditions, the DGs are required to separate from the primary network, which is known as against islanding insurance. Notwithstanding, in a high entrance level situation, in the event of a lattice issue, the course disengagement of all DGs could trigger more serious lattice issues than the underlying occasion, e.g., voltage flash, power blackouts and other force quality issues [1]. To address these expected issues, a few nations have refreshed their matrix codes for low-or medium-voltage applications to have the DGs working in a more dynamic job, giving subordinate administrations, for example, dynamic/responsive force adjustment in light of voltage/recurrence varieties and low voltage ride through (LVRT) ability. LVRT is the capacity of DG stays associated with the network all through brief period during voltage droops, and might be required to all the while proceed providing associated stacks and infuse receptive force (i.e., volt- VAR work) to lessen plausibility of voltage breakdown. For instance, the German lattice code requires responsive power infusion under flaws [3]. In Italy, the DG units associated with low-voltage matrix with their capacity rating surpassing 11.08 kW must perform LVRT support [4]. As of late, IEEE Std. 1547-2018 has included framework support capacities, similar to: ability of effectively directing voltage, ride through strange voltage/recurrence, and give inertial



reaction [5]. Moreover, Japan and different nations are attempting to audit their present lattice guidelines to oblige more dispersed force frameworks [6]. In the light of the past conversation, numerous LVRT systems have been proposed to improve the DG activity during the voltage lists [7-14]. The creators of [7] propose a voltage bolster control calculation dependent on setting the qualities for both the receptive force reference and the variable proportion among positive and negative grouping receptive current. The calculation is handled with a rearranged impedance model that requires the information on line impedance. Since the proposition considers just balanced voltage lists, the creators of [8] expand the thought for a voltage droop directing the most extreme and least stage voltages at the point of basic coupling. At last, in the two proposition, the flows are controlled in the  $\alpha\beta$  reference outline. The creators of [9] propose a control technique for PV inverters that ensures least pinnacle flows during the voltage list dodging undesirable DG separation due to overcurrent. In any case, the pinnacle current decrease is performed through current symphonious infusion, which is far from being obviously true whether it is satisfactory for voltage droops. In [10], the creators target diminishing the negative-arrangement voltage term while boosting the positive-succession voltage part. As an outcome, the lattice voltage unbalance is cut down. So as, this proposition meets LVRT prerequisites giving dynamic and responsive current without surpassing as far as possible.

Thus, this paper proposes different methods to implement active/reactive power injection control strategies on three-phase four-wire DG systems considering the natural ( $abc$ ) reference frame. The addressed strategies are: constant average active power control, constant active current control, and constant peak current control. They are characterized by setting specific percentage goals for apportioning active and reactive power during the sag. The main paper's goal is to distinguish the strategy that, considering commercial IGBT modules, better exploits the DG under voltage sag operation. The evaluation is done using the following quantifiers: 1) ratio of inverter rated power to nominal power of PES ( $A_N^{inv}/P_N$ ); 2) ratio of current rating of inverter to nominal current of the PES reflected to AC side ( $I_N^{inv}/I_N$ ); and 3) ratio of output power to maximum available power at PES ( $P_{out}/P_{mppt}$ ). Therefore, this paper contributes with:

- devise algorithms to improve LVRT and grid support for three-phase four-wire inverters in the  $abc$ -frame;
- compare constant average active power, constant active current and constant peak current strategies in terms of converter design and thermal stress;
- discuss grid-tied inverter design under fault events considering commercial IGBT modules. Simulation results are obtained from a Matlab/Simulink model using a three-phase four-wire DG system under voltage sag disturbances. This paper is an extended version of [16], emphasizing the converter design analyzes, control strategies operation under asymmetrical voltage sag, and presenting further results and discussions considering various settings for short-circuit ratio and X/R ratio.

## II. THREE-PHASE FOUR-WIRE INVERTER CONTROL

Three-stage four-wire inverters have been called attention to as one of the most reasonable geographies for applications in unequal frameworks including: appropriated age in both lattice associated and independent activity conveying highqualitypower; shunt dynamic force channels redressing ounds, unbalance, and responsive capacity to keep up sinusoidal source flows; dynamic voltage restorers (DVRs) giving voltage backing to touchy burdens during voltage lists, swells, and unbalances; among numerous others [18,19]. The rearranged graph of the three phase four-wire inverter is appeared in Fig. 1. It is part into four primary hinders: a current reference generator, a current control inder, a DC voltage control square, and heartbeat width modulator (PWM) modulator. The external voltage regulator controls the DC voltage, keeping the force balance between the converter AC and DC sides. The yield sign of the DC voltage regulator copies a comparable conductance,  $G$ , that is duplicated by standardized voltage signals,  $s^*a$ ,  $s^*b$ ,  $s^*c$ , used to shape the current references, as delineated in Fig. 2. The current reference generator ascertains the current references,  $i^*abcn$ , through the conditions depict in Section III, utilizing the deliberate stage voltages,  $v_m$ ; greatest accessible force from the essential vitality source (PES),  $P_{mppt}$  [2]; ostensible framework top voltage,  $V_N$ ; what's more, ostensible intensity of PES,  $P_N$ . The inward current control circle is contrived utilizing four relative essential (PI) regulators that create the adjusting signs to PWM



dependent on the blunders between the current references ( $I^*_{abc} = i^*_{bc} + G \cdot s^*_{abc}$ ), and the deliberate flows through the inductors ( $i_{abc}$ ), as appeared in Fig. 2. The nonpartisan current reference  $i^*_n$  is determined through Kirchoff's

current source. This latter is driven by the DC voltage closed control loop, as shown in Fig. 2.

### III. POWER INJECTION STRATEGIES

#### A. Operating ranges

In the normal operation mode, the active power reference is the output of the maximum power point tracking (MPPT) algorithm,  $P_{mppt}$ , and the system shall operate at unity powerfactor. When a voltage sag is detected, the DG runs into the LVRT operating mode, and the system is required to withstand the voltage drop for a specific period of time. Simultaneously, the converter injects a specific amount of reactive power to

$$\begin{cases} \frac{I_{rm}}{I_N} = 0 & V_{pu} > 0.9 \\ \frac{I_{rm}}{I_N} = k(1 - V_{pu}) & 0.9 \geq V_{pu} > 0.5 \\ \frac{I_{rm}}{I_N} = 1 & V_{pu} \leq 0.5 \end{cases} \quad (1)$$

where  $(I_{rm} / I_N)$  is the ratio of peak value of reactive current injection per  $m$ -phase to the nominal current of PES reflected to AC side,  $I_N = 2 \cdot \frac{P_N}{3V_N}$ ;  $V_{pu}$  is the per unit value of the grid voltage during the disturbance from its nominal value, per phase; and  $k$  is a constant given by  $k = 2$ . Then, three different operating ranges are set: (i) the normal operation from 0.9 to 1.1 p.u.; (ii) the second range is set between 0.5 to 0.9 p.u.; and (iii) the third range for voltage values lower than 0.5 p.u..

#### B. Constant Average Active Power

To maximize the active power injection of DGs, this strategy keeps the average active power constant under the disturbance. Then, the references of active ( $i^*_{am}$ ) and reactive ( $i^*_{rm}$ ) current during the voltage sag are given as following. Such that the variables  $V_{p11m}$  and  $\hat{V}_{p11m}$  shape the current reference in-phase and in-quadrature to the  $m$ -phase voltage, once the inverter control scheme is devised in  $abc$ -frame.

**Range 1 - 0.9p.u.  $\leq V_m < 1.1$  p.u**

$$\begin{cases} i^*_{am} = \frac{2(P_{mppt})}{3} \cdot \frac{1}{V_{pu}} \cdot V_{p11m} \\ i^*_{rm} = 0 \end{cases} \quad (2)$$

**Range2\_0.5 p.u.  $\leq V_m < 0.9$  p.u.**

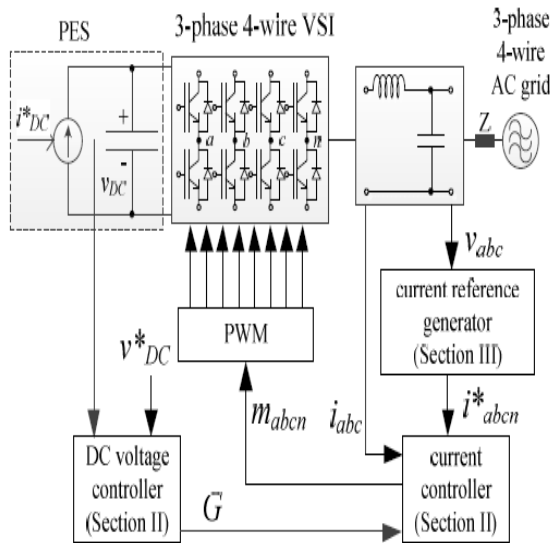


Fig. 1. Simplified diagram of the three-phase four-wire inverter and its control scheme.

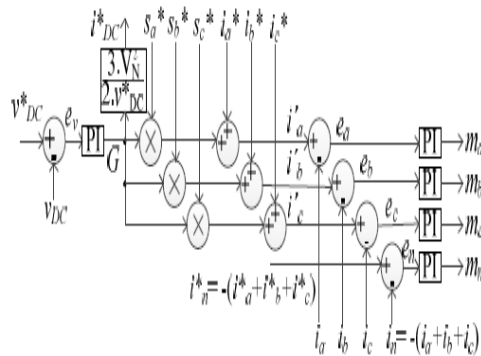


Fig. 2. Simplified block diagram of the current and voltage control scheme.

current law as  $i^*_n = -(i^*_a + i^*_b + i^*_c)$ . The system operates in closed control loop, and the PWM drives the inverter to synthesize the inductor currents accurately following the calculated current references,  $i^*_{abc}$ . The PI controllers are designed based on [22]. Finally, the converter DC side is modeled by a capacitor in parallel to a controlled



$$\begin{cases} i_{am}^* = \frac{2(P_{mppt})}{3V_N} \\ i_{rm}^* = k \cdot (1 - V_{pu}) \cdot \frac{2 \cdot P_N}{V_N} \hat{V}_{p11m} \end{cases} \quad (3)$$

Range 3 -  $V_m < 0.9$  p. u.

$$\begin{cases} i_{am}^* = \frac{2(P_{mppt})}{3V_N} \frac{1}{V_{pu}} \cdot V_{p11m} \\ i_{rm}^* = \frac{2 \cdot P_N}{V_N} \hat{V}_{p11m} \end{cases} \quad (4)$$

### C. Constant Active Current

The objective of this control strategy is provide constant active current during the voltage sag. Then, the references of active and reactive current are given as:

Range1\_0.9 p.u. ≤  $V_m < 1.1$  p. u.:

$$\begin{cases} i_{am}^* = \frac{2(P_{mppt})}{3V_N} \cdot V_{p11m} \\ i_{rm}^* = 0 \end{cases} \quad (5)$$

Range2\_0.5 p.u. ≤  $V_m < 0.9$  p. u.

$$\begin{cases} i_{am}^* = \frac{2(P_{mppt})}{3V_N} V_{p11m} \\ i_{rm}^* = k \cdot (1 - V_{pu}) \cdot \frac{2 \cdot P_N}{V_N} \hat{V}_{p11m} \end{cases} \quad (6)$$

Range 3 -  $V_m < 0.9$  p. u.

$$\begin{cases} i_{am}^* = \frac{2(P_{mppt})}{3V_N} V_{p11m} \\ i_{rm}^* = \frac{2 \cdot P_N}{V_N} \hat{V}_{p11m} \end{cases} \quad (7)$$

### D. Constant Peak Current

This control strategy establishes constant magnitude of the injected current during the voltage sag. Then, the references of active and reactive current are given as following:

Range1\_0.9 p.u. ≤  $V_m < 1.1$  p. u.:

$$\begin{cases} i_{am}^* = \frac{2(P_{mppt})}{3V_N} \cdot V_{p11m} \\ i_{rm}^* = 0 \end{cases} \quad (8)$$

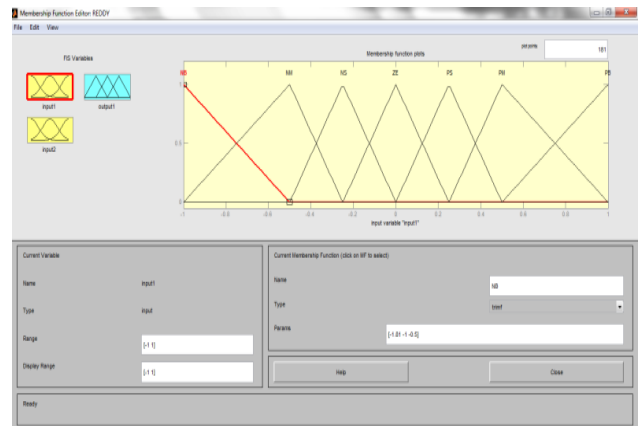
Range2\_0.5 p.u. ≤  $V_m < 0.9$  p. u.

$$\begin{cases} i_{am}^* = \sqrt{\left(\frac{P_{mppt}/3}{P_N}\right)^2 - K^2(1 - V_{pu})^2} \cdot \frac{2 \cdot P_N}{V_N} \cdot V_{p11m} \\ i_{rm}^* = k \cdot (1 - V_{pu}) \cdot \frac{2 \cdot P_N}{V_N} \hat{V}_{p11m} \end{cases} \quad (9)$$

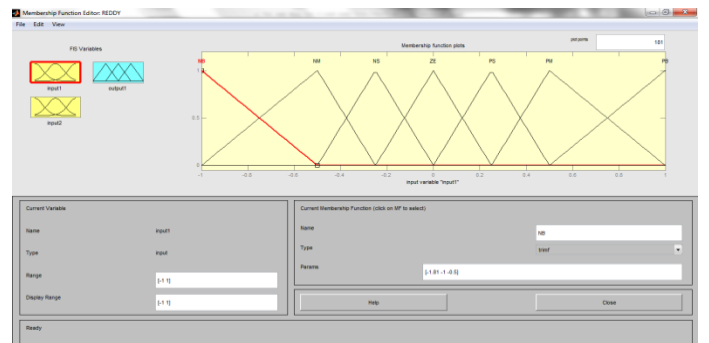
Range 3 -  $V_m < 0.9$  p. u.

$$\begin{cases} i_{am}^* = 0 \\ i_{rm}^* = \frac{2 \cdot P_N}{V_N} \hat{V}_{p11m} \end{cases} \quad (10)$$

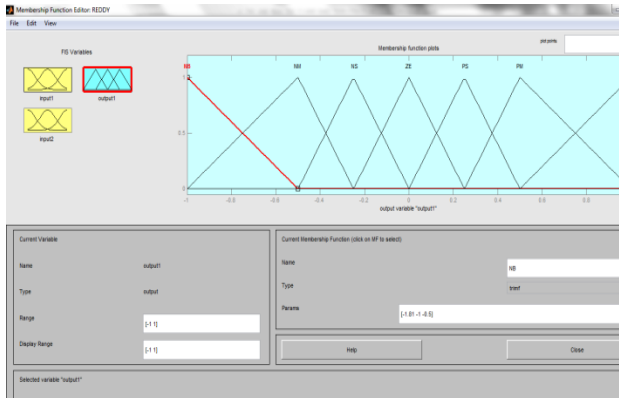
## IV. Fuzzy logic controller



### 4.1 Error



### 4.2.Change in error

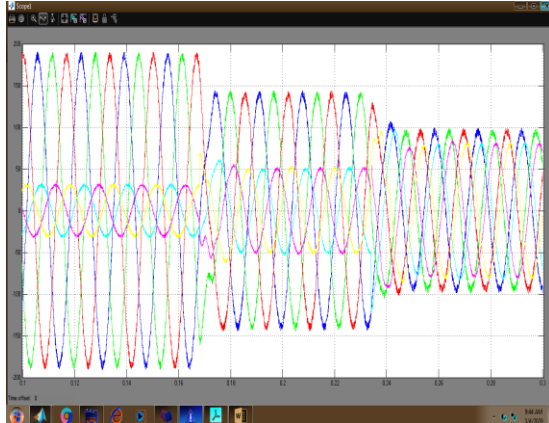


4.3.Output

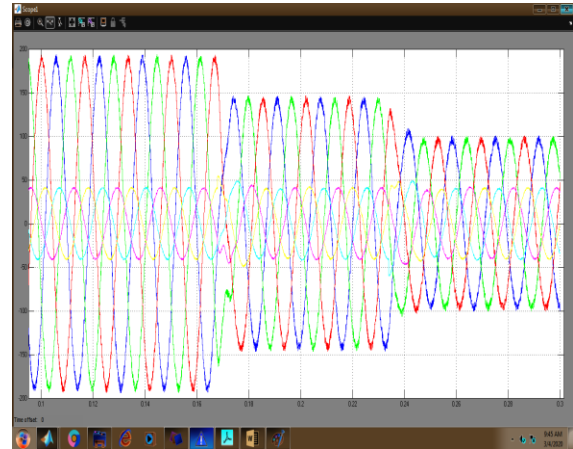
E/Δe	NB	NM	NS	ZE	PS	PM	PB
NB	ZE	NB	NB	NB	NM	NS	ZE
NM	NB	NB	NB	NM	NS	ZE	PS
NS	NB	NB	NM	NS	PS	PM	PB
ZE	NB	NS	ZE	ZE	PS	PM	PB
PS	NM	NS	ZE	ZE	PM	PB	PB
PM	ZE	ZE	PS	PS	PB	PB	PB
PB	ZE	PS	PM	PB	PB	PB	PB

V.Simulation results

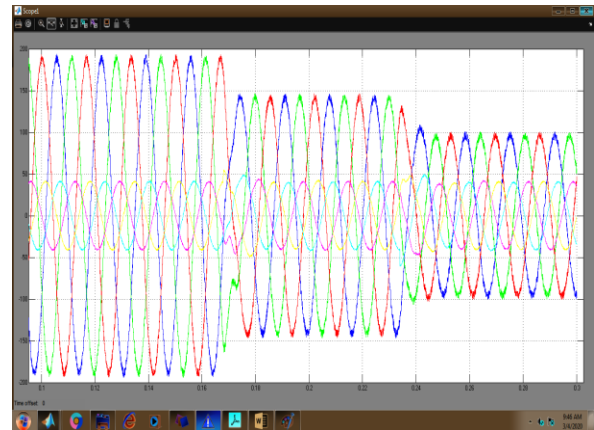
Performance of a 12 kW three-phase DG system under low voltage ride through for each control strategy (inverter current and voltage waveforms: voltage range 2 = 0.75 p.u. at  $t = 0.168s$  and voltage range 3 = 0.45 p.u. at  $t = 0.234s$ ). Performance of a 12 kW three-phase DG system under low voltage ride through for each control strategy (inverter current and voltage waveforms: voltage range 2 = 0.75 p.u. at  $t = 0.168s$  and voltage range 3 = 0.45 p.u. at  $t = 0.234s$ ).



5.1 Vgabc,Igabc of constant average active power strategy

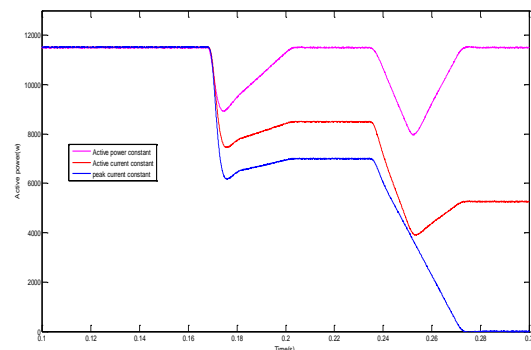


5.2 Vgabc,Igabc of constant active current strategy



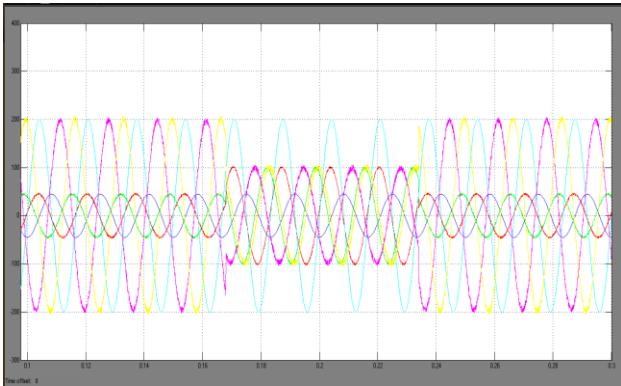
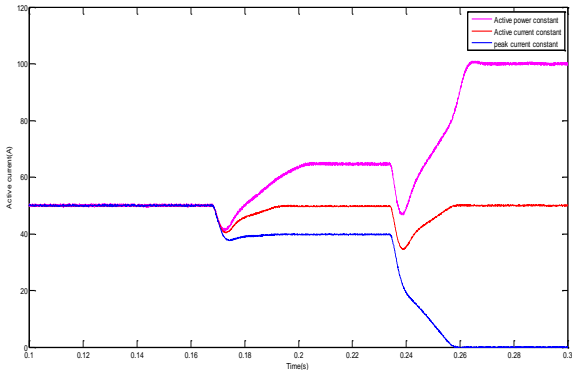
5.3 Vgabc,Igabc of constant peak current strategy

Performance of the system under low voltage ride through with the three active/reactive power injection strategies (voltage range 2 = 0.75 p.u. at  $t = 0.168s$  and voltage range 3 = 0.45 p.u. at  $t = 0.234s$ ).

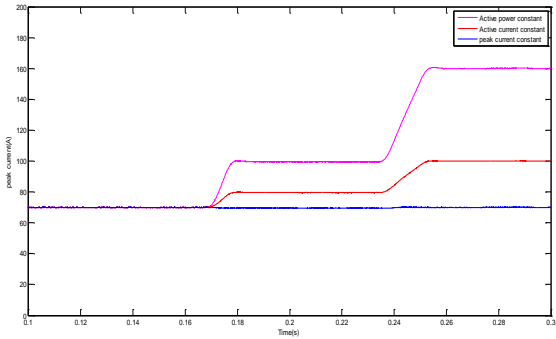




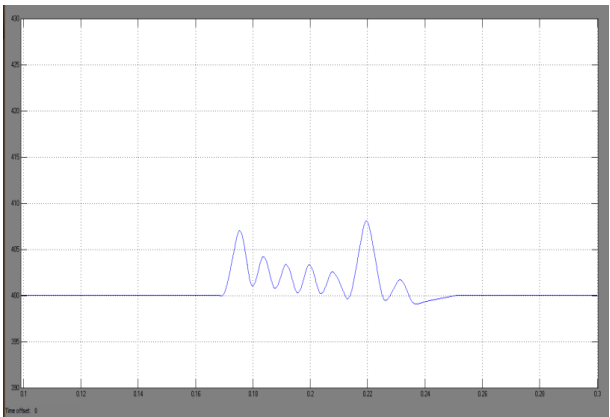
5.4 constant average active power



5.5 constant active current magnitude

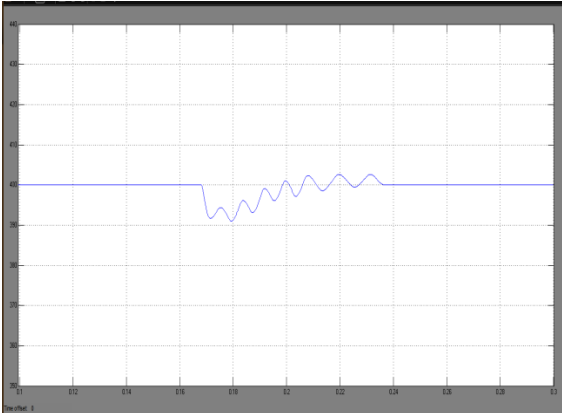


5.8 Constant average active power strategy

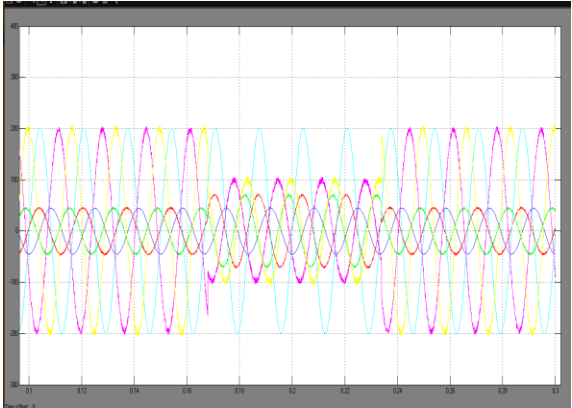


5.6 constant peak current

Characteristics of the phase voltage and current waveforms under voltage sag type E affecting phases *b* and *c* for each power injection strategy (i.e., voltage sag of 50 %).

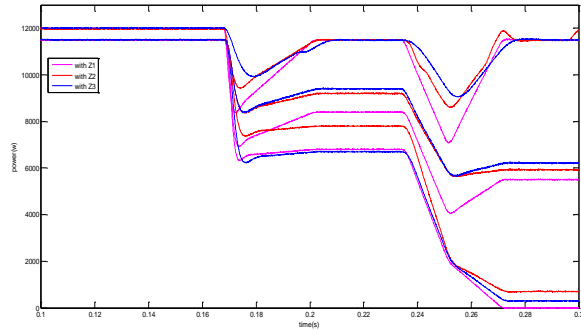


5.9 Dc link voltage (vdc)

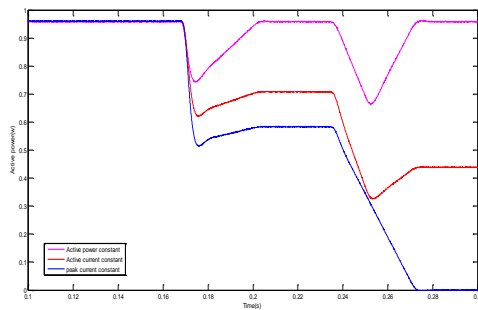


5.7 Dc link voltage (Vdc)

5.10 constant active current control



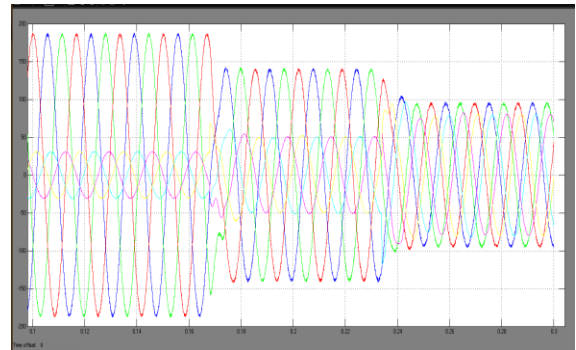
5.11 Injected active power for every power injection strategy considering the three grid impedances and varying  $V_{pu}$ .



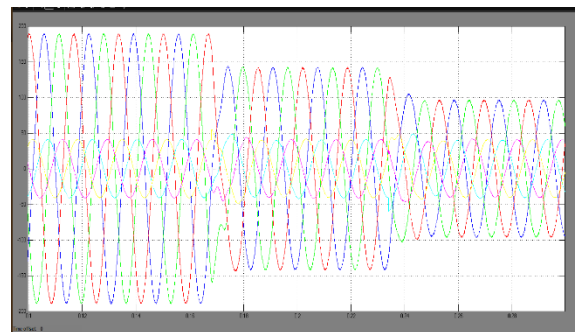
5.12. Comparative of the three power injection strategies in terms of the active power injected factor ( $P / P_N$ ) during voltage sags

**Simulation results by using fuzzy logic controller**

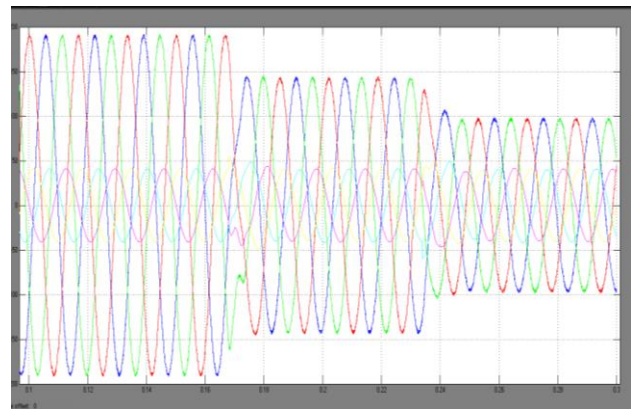
Performance of a 12 kW three-phase DG system under lowvoltage ride through for each control strategy (inverter current andvoltage waveforms: voltage range 2 = 0.75 p.u. at  $t = 0.168s$  andvoltage range 3 = 0.45 p.u. at  $t = 0.234s$ ).



5.13 constant average active power strategy



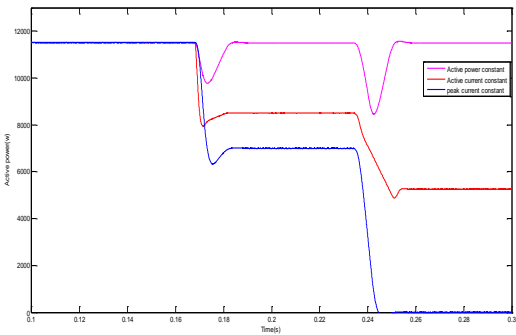
5.14 constant active current strategy



5.15 constant peak current strategy

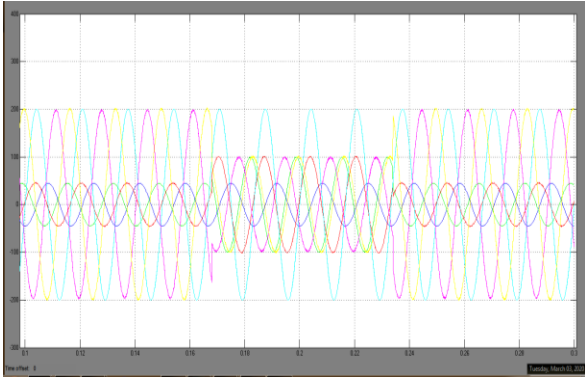


phases b and c for each powerinjection strategy (i.e., voltage sag of 50 %).

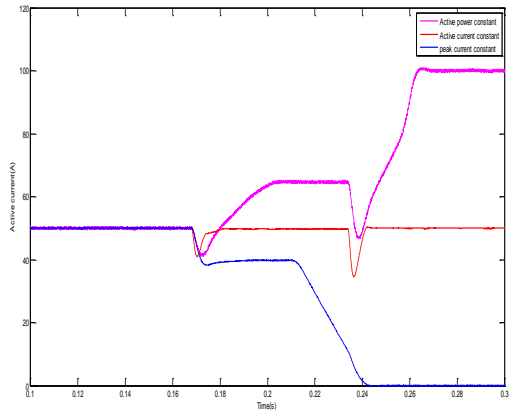


5.16 constant average active power

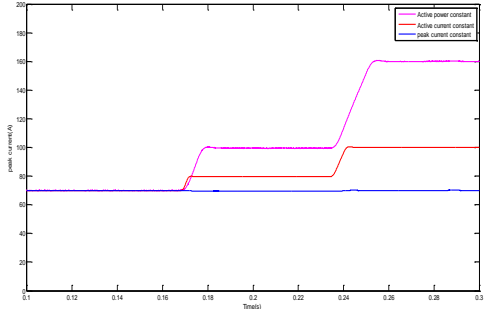
Performance of the system under low voltage ride through with the three active/reactive power injection strategies (voltage range 2 = 0.75 p.u. at t = 0.168s and voltage range 3 = 0.45 p.u. at t = 0.234s).



5.19 constant average active power strategy

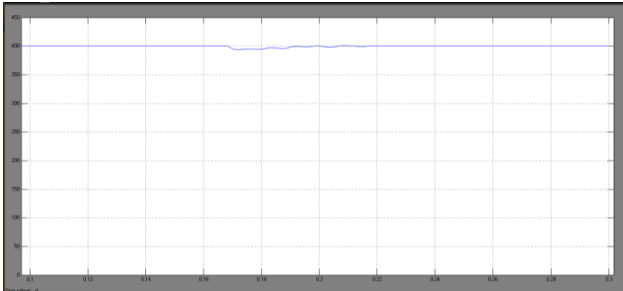


5.17 constant active current magnitude

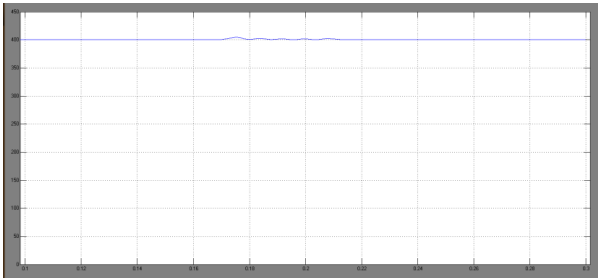


5.18 Constant peak current

Characteristics of the phase voltage and current waveforms under voltage sag type E affecting

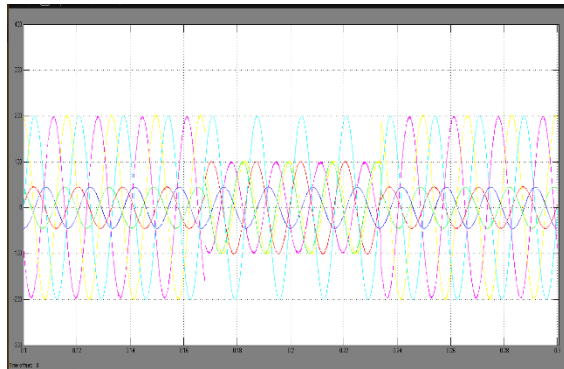


5.20 Dc link voltage (Vdc) (a)

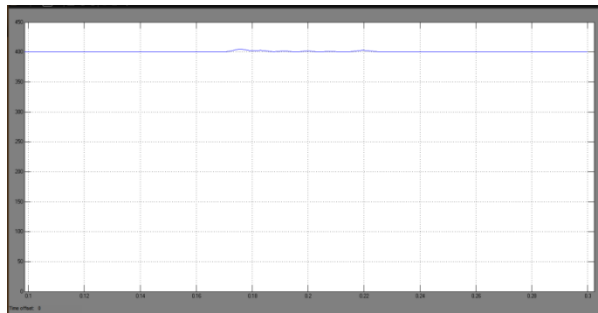


5.21 dc link voltage

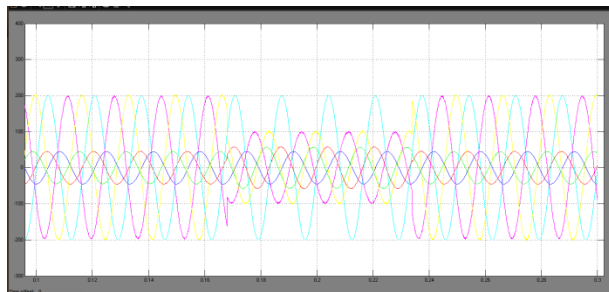




5.22 constant active current control



5.23 dc link voltage



5.24 constant peak current control

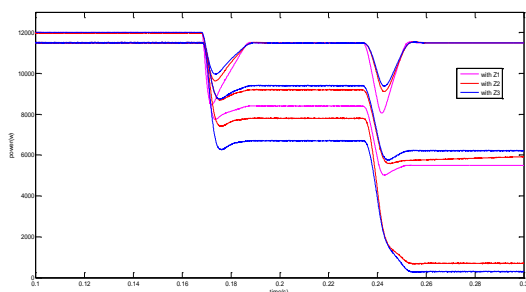


Fig.5.25. Injected active power for every power injection strategy considering the three grid impedances and varying  $V_{pu}$ .

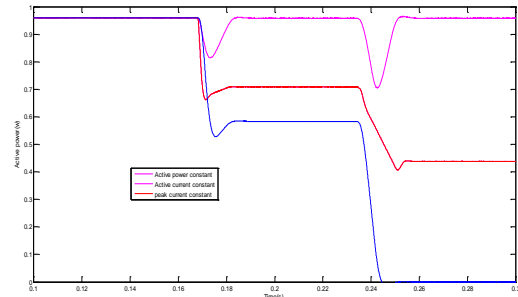


Fig. 5.26 Comparative of the three power injection strategies in terms of the active power injected factor ( $P / P_N$ ) during voltage sags with the converter properly re-designed according to  $I_N$  ratio.

## VI. CONCLUSIONS

In this paper it proposes a power injection strategies for three\_phase four\_wire inverters during symmetrical/asymmetrical voltage sags by using fuzzy logic controller. The power infusion systems include consistent normal dynamic power, steady dynamic current, and consistent pinnacle current. These systems were thought about and broke down regarding converter power/current measuring, decrease in dynamic force infusion because of voltage list, required receptive current infusion, and DC-interface voltage swaying under lopsided voltage list, and short out variety. To meet lattice code prerequisites of receptive force infusion under voltage aggravations, and furthermore to all the more likely endeavor the dynamic over infusion. For monetarily accessible IGBT modules (i.e., high power factor), the diode warm opposition is normally twice the semiconductor warm opposition, which implies that for an DC/AC inverter handling dynamic/responsive force the diodes withstand lower estimation of current than the inverter's semiconductor as a result of their relating chip territory. At that point, the inverter must be planned dependent on the diode warm cutoff points, and the semiconductor will be normally curiously large. Along these lines, among the dissected infusion systems the best one is the steady normal force with current reduction instrument up to the semiconductor current rating.



## REFERENCES

- [1] Y. Yang, P. Enjeti, F. Blaabjerg and H. Wang, Wide-Scale Adoption of Photovoltaic Energy: Grid Code Modifications are Explored in the Distribution Grid IEEE Industry Applications Magazine, vol. 21, no. 5, pp. 21-31, Sept.-Oct. 2015.
- [2] M. A. G. de Brito, L. Galotto, L. P. Sampaio, G. d. A. e Melo and C. A. Canesin, Evaluation of the Main MPPT Techniques for Photovoltaic Applications, IEEE Transactions on Industrial Electronics, vol. 60, no. 3, pp. 1156-1167, March 2013.
- [3] Y. Yang, P. Enjeti, F. Blaabjerg and H. Wang, suggested grid code modifications to ensure wide-scale adoption of photovoltaic energy in distributed power generation systems, 2013 in IEEE Industry Applications Society Annual Meeting, Lake Buena Vista, FL, 2013, pp. 1-8.
- [4] Comitato Elettrotecnico Italiano, Reference Technical Rules for Connection of Active and Passive users to the LV Electrical Utilities, CEI 0-21, July. 2016.
- [5] IEEE Standards Coordinating Committee 21, IEEE Standard for Interconnection and Interoperability of Distributed Energy Resource with Associated Electric Power Systems Interface., 2018.
- [6] H. Kobayashi, Fault ride through requirements and measures of distributed PV systems in Japan," in IEEE Power and Energy Society General Meeting, San Diego, CA, 2012, pp. 1-6.
- [7] J. Miret, A. Camacho, M. Castilla, L. García de Vicuña, and J. Matas, Control scheme with voltage support capability for distributed generation inverters under-voltage sags, IEEE Transaction on Power Electronics, vol. 28, no. 11, pp. 5252–5262, Nov. 2013.
- [8] A. Camacho, M. Castilla, J. Miret, R. Guzman, and A. Borrell, Reactive power control for distributed generation power plants to comply with voltage limits during grid faults, IEEE Transaction on Power Electronics, vol.29 no. 11, pp. 2624–2634, Nov. 2014
- [9] J. Miret, M. Castilla, A. Camacho, L. García de Vicuña, and J. Matas, Control scheme for photovoltaic three-phase inverters to minimize peak currents during unbalanced grid-voltage sags, IEEE Transaction on Power Electronics, vol. 27, no. 10, pp. 4262–4271, Oct. 2012.
- [10] C. Lee, C. Hsu and P. Cheng, A Low-Voltage Ride-Through Technique for Grid-Connected Converters of Distributed Energy Resources, in IEEE Transactions on Industry Applications, vol. 47, no. 4, pp. 1821-1832, July- Aug. 2011.
- [11] J. L. Sosa, M. Castilla, J. Miret, J. Matas and Y. A. Al-Turki, Control Strategy to Maximize the Power Capability of PV Three-Phase Inverters During Voltage Sags, IEEE Transactions on Power Electronics, vol. 31, no. 4, pp.3314-3323, April 2016.
- [12] M. A. G. Lopez, J. L. G. de Vicuna, J. Miret, M. Castilla and R. Guzman, Control Strategy for Grid-Connected Three-Phase Inverters During Voltage Sags to Meet Grid Codes and to Maximize Power Delivery Capability. IEEE Transactions on Power Electronics, early access, 2018.
- [13] Y. Yang, H. Wang and F. Blaabjerg, Reactive Power Injection Strategies for Single-Phase Photovoltaic Systems Considering Grid Requirements, IEEE Transactions on Industry Applications, vol. 50, no. 6, pp. 4065-4076, Nov.-Dec. 2014.